Differential Sensitivities of Fast- and Slow-Cycling Cancer Cells to Inosine Monophosphate Dehydrogenase 2 Inhibition by Mycophenolic Acid

Kan Chen,[1,2]* Wanlu Cao,[1]* Juan Li,[1] Dave Sprengers,[1] Pratika Y Hernanda,[3] Xiangdong Kong,[2] Luc JW van der Laan,[4] Kwan Man,[5] Jaap Kwekkeboom,[1] Herold J Metselaar,[1] Maikel P Peppelenbosch,[1] and Qiuwei Pan[1]

[1]Department of Gastroenterology and Hepatology, Erasmus MC Cancer Institute, Erasmus University Medical Center, Rotterdam, The Netherlands; [2]Bio-X Center, College of Life Sciences, Zhejiang Sci-Tech University, Hangzhou, China; [3]Laboratory of Medical Genetics, Biomolecular Research Center, Wijaya Kusuma University, Surabaya, Indonesia; [4]Department of Surgery, Erasmus University Medical Center, Rotterdam, The Netherlands; and [5]Department of Surgery, Hong Kong University, Hong Kong, China

As uncontrolled cell proliferation requires nucleotide biosynthesis, inhibiting enzymes that mediate nucleotide biosynthesis constitutes a rational approach to the management of oncological diseases. In practice, however, results of this strategy are mixed and thus elucidation of the mechanisms by which cancer cells evade the effect of nucleotide biosynthesis restriction is urgently needed. Here we explored the notion that intrinsic differences in cancer cell cycle velocity are important in the resistance toward inhibition of inosine monophosphate dehydrogenase (IMPDH) by mycophenolic acid (MPA). In short-term experiments, MPA treatment of fast-growing cancer cells effectively elicited G0/G1 arrest and provoked apoptosis, thus inhibiting cell proliferation and colony formation. Forced expression of a mutated IMPDH2, lacking a binding site for MPA but retaining enzymatic activity, resulted in complete resistance of cancer cells to MPA. In nude mice subcutaneously engrafted with HeLa cells, MPA moderately delayed tumor formation by inhibiting cell proliferation and inducing apoptosis. Importantly, we developed a lentiviral vector–based Tet-on label-retaining system that enables to identify, isolate and functionally characterize slow-cycling or so-called label-retaining cells (LRCs) in vitro and in vivo. We surprisingly found the presence of LRCs in fast-growing tumors. LRCs were superior in colony formation, tumor initiation and resistance to MPA as compared with fast-cycling cells. Thus, the slow-cycling compartment of cancer seems predominantly responsible for resistance to MPA.

INTRODUCTION

Uncontrolled cell proliferation resulting from cell cycling deregulation is a hallmark of cancer. Although aggressive cancers are diverse and heterogeneous, they almost universally contain a fast-cycling compartment that can rapidly complete a cell cycle, and these cells are primarily responsible for the increase in tumor mass (1). This impressive proliferative capacity is, however, dependent on adequate supply of nucleotides. Cellular nucleotide synthesis is biochemically complex, but requires various enzymes that can be targeted clinically, including inosine monophosphate dehydrogenase (IMPDH), which is a rate-limiting enzyme in *de novo* synthesis of guanine.

The enzymatic activity of IMPDH is composed of two separate isoforms, type 1 and 2 (2). The IMPDH2 isoform is associated with aggressive cancerous disease in experimental cancer (3–6), and related to poor survival in osteosarcoma patients (7). Mycophenolic acid (MPA) acts as a nonnucleoside, noncompetitive, reversible inhibitor of IMPDH with fivefold higher potency of inhibiting IMPDH2 than IMPDH1. It has been reported to be able to inhibit cancer cell proliferation and induce apoptosis in several experimental models of human solid tumors and hematological malignancies by depleting guanine nucleotide pools (5,8–10).

In the last decade, interest into the importance of cell cycle velocity heterogeneity of cancers has increased. Although it was initially thought that

*KC and WC contributed equally to this work.

Address correspondence to Qiuwei Pan, Department of Gastroenterology and Hepatology, Erasmus MC, room Na-617, 'sGravendijkwal 230, NL-3015 CE Rotterdam, The Netherlands. Phone: +31-(0)107037502; Fax: +31-(0)107032793; E-mail: q.pan@erasmusmc.nl.

cancer cells universally cycle and grow faster than normal cells, recently a slow-cycling (largely quiescent) compartment, which does not divide frequently but has the capacity to generate progeny that can repopulate the fast cycling compartment, has been identified in many tumors, (11). Functionally, these slow-cycling cancer cells appear to be associated with the capacity to generate new metastases while having superior resistance to therapy (12). Technically, these slow-cycling cells are identified by their capacity to retain a pulse label as faster cycling cells lose the pulse label at cell division. Thus these cells are indicated with the term label-retaining cells (LRCs) (13).

In this study, we aim to develop a lentiviral vector–based Tet-on label-retaining system that allows us to identify slow-cycling cancer cells *in vivo,* so that they can be subsequently isolated for functional characterization. We exploit this system to investigate the different sensitivity between fast- and slow-cycling cancer cells to IMPDH2 inhibition by MPA.

MATERIALS AND METHODS

Reagents

Stocks of MPA (AMRESCO LLC) were dissolved in dimethyl sulfoxide (DMSO) (Sigma-Aldrich). Doxycycline, collagenase IV and DNase were purchased from Sigma-Aldrich Corporation. Antibodies against IMPDH2, p-Histone3 and cleaved caspase-3 were purchased from Abcam Company, Millipore Corporation and Cell Signaling Technology, respectively.

Cell Culture

To investigate the effects of MPA on cancer cells, seven different cancer cell lines derived from various tumor types were cultured. Human hepatoma cell lines HepG2 and HuH7, colon adenocarcinoma cell line Caco2, the epithelioid cervix carcinoma cell line HeLa and ovary adenocarcinoma cell line SKOV-3 were grown in Dulbecco's modified Eagle medium (DMEM) (GIBCO, Life

Technologies). Pancreatic cancer cell lines BxPC3 and PANC-1 were cultured with RMIP-1640. Both of the mediums were supplemented with 10% (v/v) fetal bovine serum (FBS) (Hyclone Technologies), 100 units/mL of penicillin and 100 μg/mL of streptomycin. All the cells were incubated at 37°C in a humidified atmosphere containing 5% CO_2. All the cell lines were confirmed mycoplasma free and their STR genotyping was analyzed at the Department of Pathology, Erasmus Medical Center Rotterdam (Supplementary Table S1).

Lentiviral Vector–Based Tet-On Label-Retaining System

Lentiviral backbone plasmids pLV. EX3D/EF1A-rtTA (M2)-dsRed-Express2 and pLV.EX2D/TRE-eGFP were used to pack third generation lentiviral vectors (Supplementary Figure S1A). HeLa cells were transduced with both vectors to generate a system (HeLa Tet-on) that can express a histone 2B-green fluorescent fusion protein (histone-GFP) upon induction by doxycycline. GFP expression *in vitro* was analyzed from wk 0 to wk 3 by flow cytometry analysis (FACS) and confocal microscope (Zeiss LSM 510) (Supplementary Figures S1B,C). ZenlightEdition software was used to analyze confocal microscope images. Cells that maintained GFP expression over this period of time were identified as LRCs.

For identification of LRCs *in vivo*, female NOG mice at the age of 8 to 10 wks were purchased from Taconic Biosciences (Denmark). Animal experiments were performed with the approval of the institutional animal ethics committee (Dier Experimenten Commissie, Erasmus MC). Mice were bred in a special pathogen free (SPF) environment during the whole experimental period. Mice were injected subcutaneously with 5×10^6 HeLa Tet-on cells. After engraftment (10 to 15 d), water containing 1 mg/mL doxycycline and 5% sucrose was given for 5 d. Mice were killed at different time points after withdrawal of doxycycline. A portion of harvested tumor samples was fixed with 4% paraformaldehyde

and embedded in paraffin for subsequent immunohistochemistry, while the remaining tumor tissue was dissociated with 5 mg/mL collagenase IV and 2 mg/mL DNase at 37°C for 30 min to obtain single cell suspension. Cells were further sorted as singlets for separation into non-LRCs (GFP^{low}dsRed) and LRCs (GFP^{high}dsRed) by FACS sorter (Supplementary Figure S2). non-LRCs and LRCs were injected subcutaneously (either 1,000 cells or 10,000 cells per injection as appropriate) on four sites in the mice. At the same time, two populations of sorted cells were plated for colony-forming unit (CFU) assay (treated with or without MPA).

Colony Formation Assay

Cells were harvested and suspended in culture medium, yields were quantified through counting and plated in 6-well plates (500 cells/well), and then treated with serial dilutions of MPA (1, 2, 3, 4 and 5 μg/mL). The control group was supplemented with an equal volume of PBS. For the cells derived from xenograft tumor, cells were seeded into 12-well collagen coating plates and cultured in medium with or without MPA (10 μg/mL). Formed colonies were fixed by 70% ethanol and counterstained with hematoxylin and eosin after two weeks. Colony numbers were counted and their sizes were measured microscopically through digital image analysis.

MTT Assay

Cells were seeded in a 96-well plate at a concentration of 5×10^3 cells/well in 100 μL medium. Cells were incubated overnight to attach to the bottom of the wells, and then treated with serials dilutions of MPA (1, 5, 10, 15, 20, 25 and 30 μg/mL). Cell viability was analyzed by adding 5 mg/mL MTT (Sigma-Aldrich) and 150 μL DMSO. Absorbance was determined using Enzyme mark instrument at the wavelength of 490 nm.

Analysis of Cell Cycle

Cells (5×10^5/well) were plated in six-well plates and allowed to attach overnight, followed by an application

of MPA at concentrations of 5, 10, 15, 20 and 25 μg/mL for 48 h. Vehicle control was performed through the addition of an equal volume of PBS. After 48 h, control and treated cells were trypsinized and washed with PBS and then fixed in cold 70% ethanol overnight at 4°C. The cells were washed twice with PBS and incubated with 20 μg/mL RNase at 37°C for 30 min, and then with 50 μg/mL propidium iodide (PI) at 4°C for 30 min. The samples were analyzed immediately by FACS. Cell cycle was analyzed by ModFit LT 3.0 software.

Analysis of Cell Apoptosis

Cell apoptosis analysis was performed by staining cells with annexin V-FITC and PI. Cells (5×10^5/well) were seeded into six-well plates and incubated at 37°C in 5% CO_2 overnight, then serial dilutions of MPA (5, 10, 15, 20 and 25 μg/mL) were added; whereas for vehicle control, an equal volume of PBS was used. After 48 h, all of the cells were trypsinized and resuspended in annexin-binding buffer and stained with Alexa Fluor 488 annexin V and PI at room temperature for 15 min. Detection of apoptosis was performed by FACS.

Xenograft Assays in Nude Mice

The xenograft tumor model was performed using nude mice in accordance with current prescribed guidelines and under a protocol approved by the Institutional Animal Care and Use Committee of Hangzhou Normal University, China. Mice were bred in an SPF environment during the whole experimental period. Mice were all female and 4 to 6 wks of age at the time of inoculation, and were subcutaneously inoculated with 5×10^6 of HeLa cells. After 20 h, mice were divided into three groups and were treated with different doses of MPA or PBS (240 mg/kg body weight, n = 10; 60 mg/kg body weight, n = 11 and PBS, n = 10) (2). MPA was injected intraperitoneally (IP) for 20 consecutive days. Tumor formation was monitored through palpation. At d 30 postengraftment, mice were killed and tumors were

harvested and macroscopically analyzed. Tumor tissues were fixed with 4% paraformaldehyde and embedded in paraffin for evaluation by histology or immunohistochemistry.

Immunohistochemistry

Paraffin-embedded tumor tissue slides were deparaffined in xylene, rehydrated in graded alcohols, and rinsed in PBS supplemented with 0.05% Tween 20. Slides were boiled in citrate acid buffer (pH 6.0) for 10 min to retrieve antigen. A 3% H_2O_2 treatment for 20 min at room temperature was used to block endogenous peroxidase activity. The slides were incubated in 5% milk-containing blocking solution followed by overnight incubation with either a rabbit monoclonal antibody against IMPDH2, a rabbit polyclonal antibody against p-Histone H3 or a rabbit polyclonal antibody against cleaved caspase-3, used at a final dilution of 1:500, 1:1000 or 1:3000, respectively, and then counterstained with hematoxylin according to routine procedures. As a negative control, the primary antibody was omitted; positive controls were taken from other slides that had been successfully stained before. IMPDH2, phospho-histone H3 and cleaved caspase-3 staining were scored by two independent expert observers. The numbers of mitotic cells and cleaved caspase-3-positive cells were counted in ten high-power fields. Median numbers of positive cells in each of the ten fields were calculated for each sample of the different groups using a semiquantitative assessment. Three categories were used to evaluate the percentages of apoptotic cells: <10%, mild; 10% to 50%, moderate; >50%, high. The intensity of IMPDH2 staining was presented by categories: + weak; + + moderate; + + + strong.

Statistical Analysis

Statistical analysis was performed by using the nonparametric Mann–Whitney test for paired or non-paired data, or the paired *t* test using GraphPad InStat software as appropriate. A *P* value < 0.05 was considered statistically significant.

All supplementary materials are available online at www.molmed.org.

RESULTS

MPA Is Very Effective for Inhibiting Cancer Cell Proliferation in Fast-Growing Cell Lines

A first indication as to how MPA affects cancer cells in relation to cell cycle velocity comes from experiments in which we investigated the effects of MPA on cell proliferation and the colony-forming potential of different cancer cell lines. To this end, seven different cancer cell lines derived from various tumor types were compared. Growth curves show substantial variation in the proliferation rate and colony-forming potential of these cell lines, with, in general, HeLa and Caco2 showing more aggressive behavior as compared with the other cell lines (Figure 1). Challenge with MPA inhibited both cell proliferation and colony unit-forming potential of cancer cell lines, but, strikingly, fast-growing cell lines are more affected by MPA treatment as compared with slow-growing cell lines (Figure 1), indicating that MPA mainly affects the fast-cycling compartment.

MPA Inhibited Cell Proliferation, Arrested Cell Cycling and Induced Cell Apoptosis in Fast-Growing Cancer Cell Line

To further understand how MPA acts on fast-growing cancer cells, HeLa cells (the most sensitive cell line to MPA from our panel of cancer cell lines) were treated with clinically relevant MPA concentrations (14) and analyzed in more detail for the effects of MPA on cellular expansion, cell cycle and programmed cell death. MPA counteracted HeLa cell proliferation and colony-forming potential in a time- and dose-dependent manner (Figure 2A). Indeed, even a relatively low concentration (1 μg/mL) of MPA already substantially impeded colony formation, whereas higher concentrations (2–5 μg/mL) completely inhibited
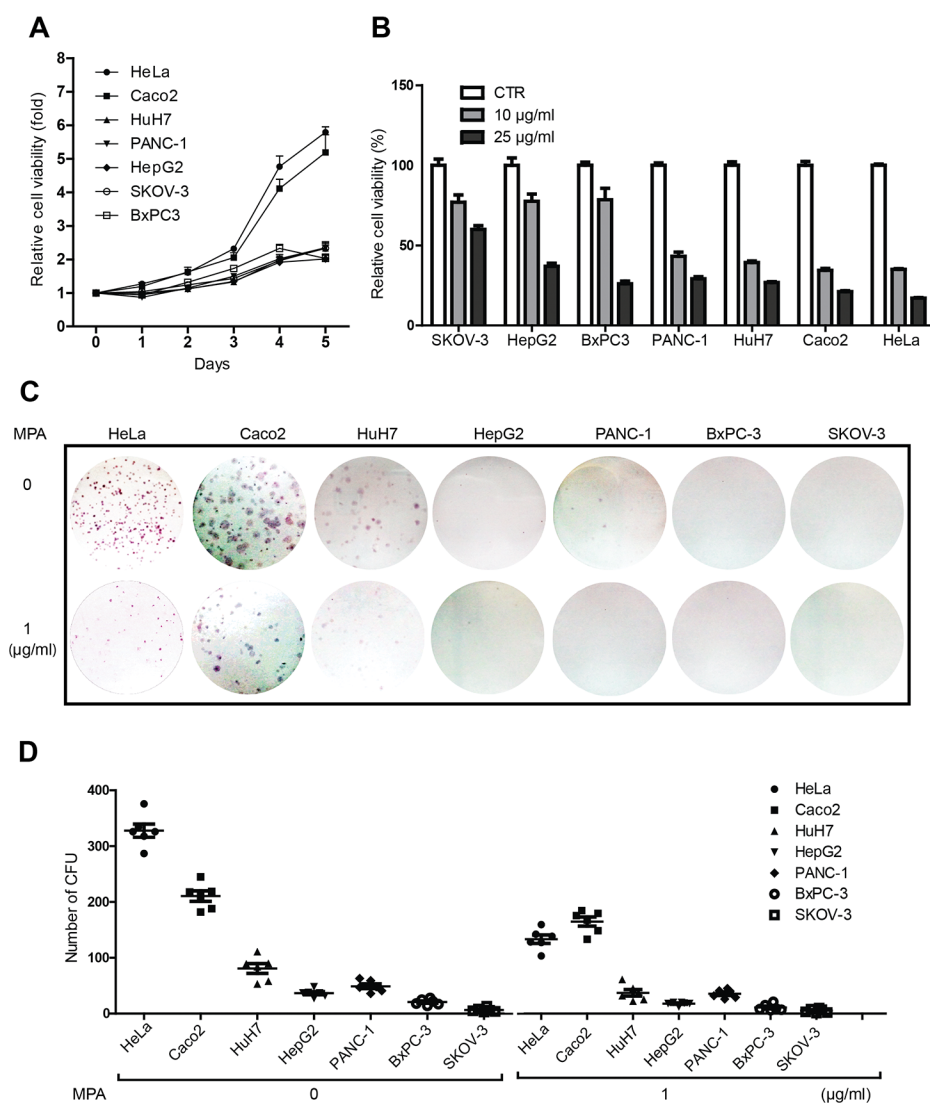
Figure 1. MPA inhibited cell proliferation and colony formation of different cancer cell lines. (A) Growth curve of seven different cancer cell lines show that HeLa cells grow faster than the other cell lines tested (mean ± SD, n = 6). (B) MPA inhibited cell proliferation of all seven cancer cell lines as determined by MTT; data shown cells were treated by MPA for 72 h (mean ± SD, n = 5). (C) and (D) MPA inhibited single cell colony formation of seven cancer cell lines (mean ± SD, n = 6, ***$P < 0.001$).

IMPDH2 Is a Relevant Target for MPA in Inhibiting Cancer Cell Growth

The clinical effects of MPA are presumed to be mediated through inhibition of IMPDH enzymatic activity and subsequent inhibition of *de novo* nucleotide biosynthesis. Although two isoforms of IMPDH exist, the type II isoform (IMPDH2) exhibits a five-fold higher sensitivity to inhibition by MPA as compared with the type I isoform (IMPDH1) (3). IMPDH2 is assumed to be the major target of MPA. Moreover, IMPDH2 is often upregulated in cancer (15), suggesting that IMPDH2 is the relevant target for MPA in the experiments described above. To substantiate this notion, we employed a lentiviral vector expressing an experimentally mutated *IMPDH2* (mut*IMPDH2*) fused to *GFP* (16,17). The product of this construct has normal IMP dehydrogenase activity but lacks the binding site for MPA and thus confers MPA resistance. Transduction of this vector resulted in successful expression of this mutated allele in HeLa cells (Figure 3A). In the CFU assay, forced expression of this mutated *IMPDH2* provoked resistance to MPA treatment (Figures 3B,C). Furthermore, the mut*IMPDH2* cells prevented MPA-induced apoptosis (Figure 3D). These results are consistent with a key role of IMPDH2 in mediating the effects of MPA in our experimentation.

MPA Delayed Tumor Initiation, Inhibited Cancer Cell Proliferation and Induced Cell Apoptosis *In Vivo*

Insight into the effects of MPA on tumor cell *in vivo* was obtained in experiments in which nude mice were used for subcutaneous engraftment of the HeLa cell line. Twenty h after inoculation, mice were injected IP with MPA for 20 consecutive days. In this xenograft model, treatment of MPA (60 mg/kg body weight) significantly ($P < 0.05$) delayed tumor initiation (Figure 4A). In the 240-mg/kg body weight of the MPA-treated group, one mouse failed to form a tumor; while tumor formation also tended to be
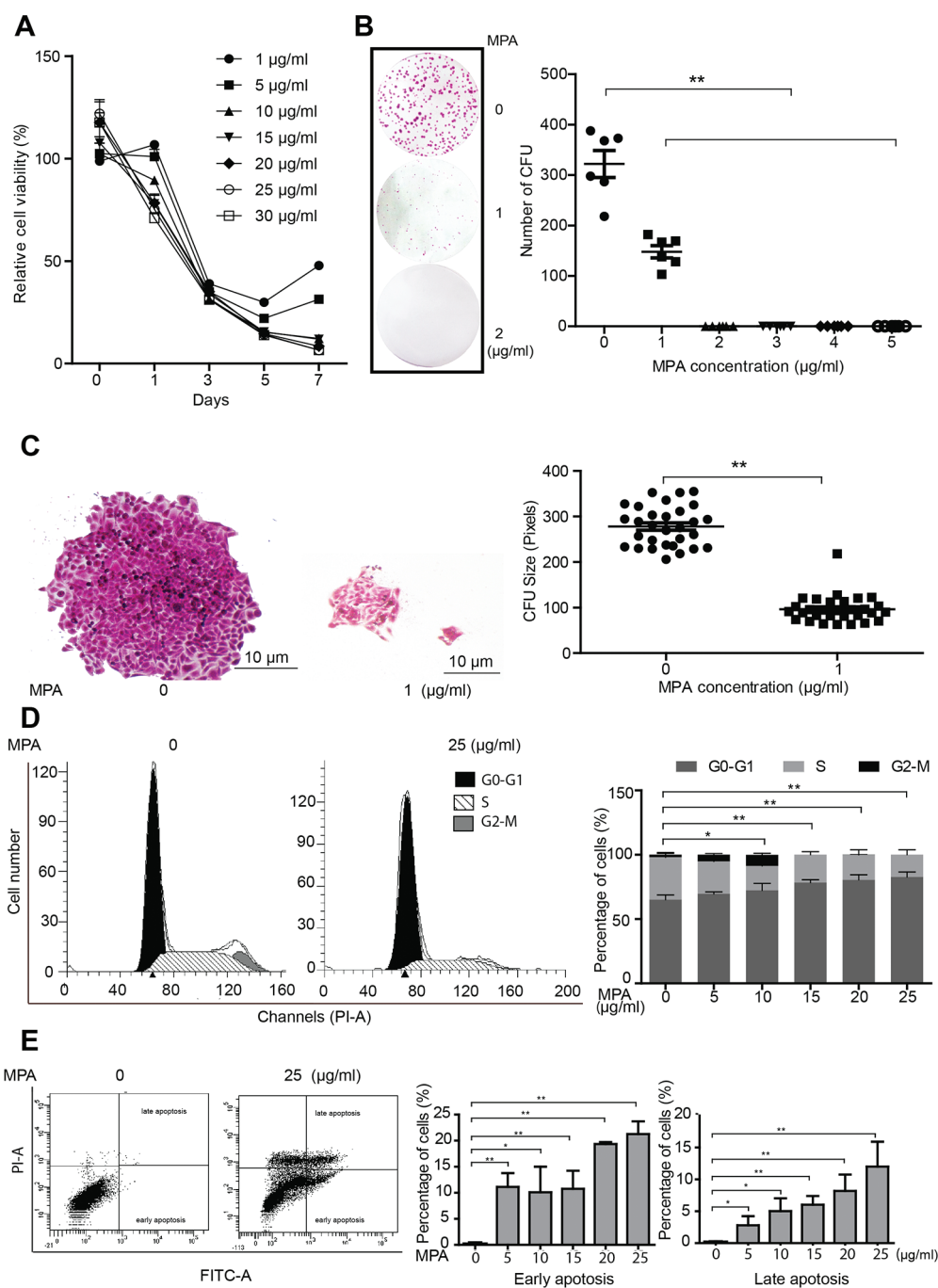
colony formation. The result reports 322 ± 27 colonies/500 cells were formed in untreated group, but only 148 ± 27 colonies were formed in 1 μg/mL MPA-treated groups (mean ± SEM, n = 6, $P < 0.01$) (Figure 2B). Accordingly, the size of CFUs was significantly smaller in MPA-treated groups compared with untreated groups (96 ± 5 pixels versus 278 ± 8 pixels, mean ± SEM, n = 30,

$P < 0.01$) (Figure 2C). Furthermore, MPA dose-dependently provoked the G0/G1-phase arrest (Figure 2D). In addition, MPA dose-dependently triggered both early and late cell apoptosis (Figure 2E). These data suggest that MPA profoundly interferes with the physiology of fast-growing cancer cells and raises questions as to how cancers can escape the effects of MPA.

Figure 2. MPA counteracts proliferation of a fast-growing cancer cell line. (A) Clinically-relevant MPA concentrations potently inhibit proliferation of the HeLa cell line as assessed by MTT activity (mean ± SD, n = 5). (B) Clinically-relevant MPA concentrations impair colony formation of HeLa cells (mean ± SD, n = 6). (C) Clinically-relevant MPA concentrations impair colony growth of HeLa cell as determined by image analysis (mean ± SEM, n = 30, **$P < 0.01$). (D) MPA treatment causes G0/G1 phase cell cycle arrest. The left panel shows cell cycle phase distribution of a vehicle-treated culture, whereas the middle panel shows cell cycle phase distribution in a MPA-treated culture. The right panel shows a quantification of the MPA effects on the cell cycle of HeLa (mean ± SD, n = 3. *$P < 0.05$; **$P < 0.01$). (E) FACS analysis of cellular apoptosis through annexin-V positivity and PI incorporation. The left panel provides an example of a vehicle-treated HeLa culture, whereas the middle panel provides an example of the effects seen following MPA treatment. The quantification in the right panel shows statistically significant stimulation of both early and late apoptosis in the 5–25 μg/mL MPA concentration (mean ± SD, n = 3, *$P < 0.05$; **$P < 0.01$).
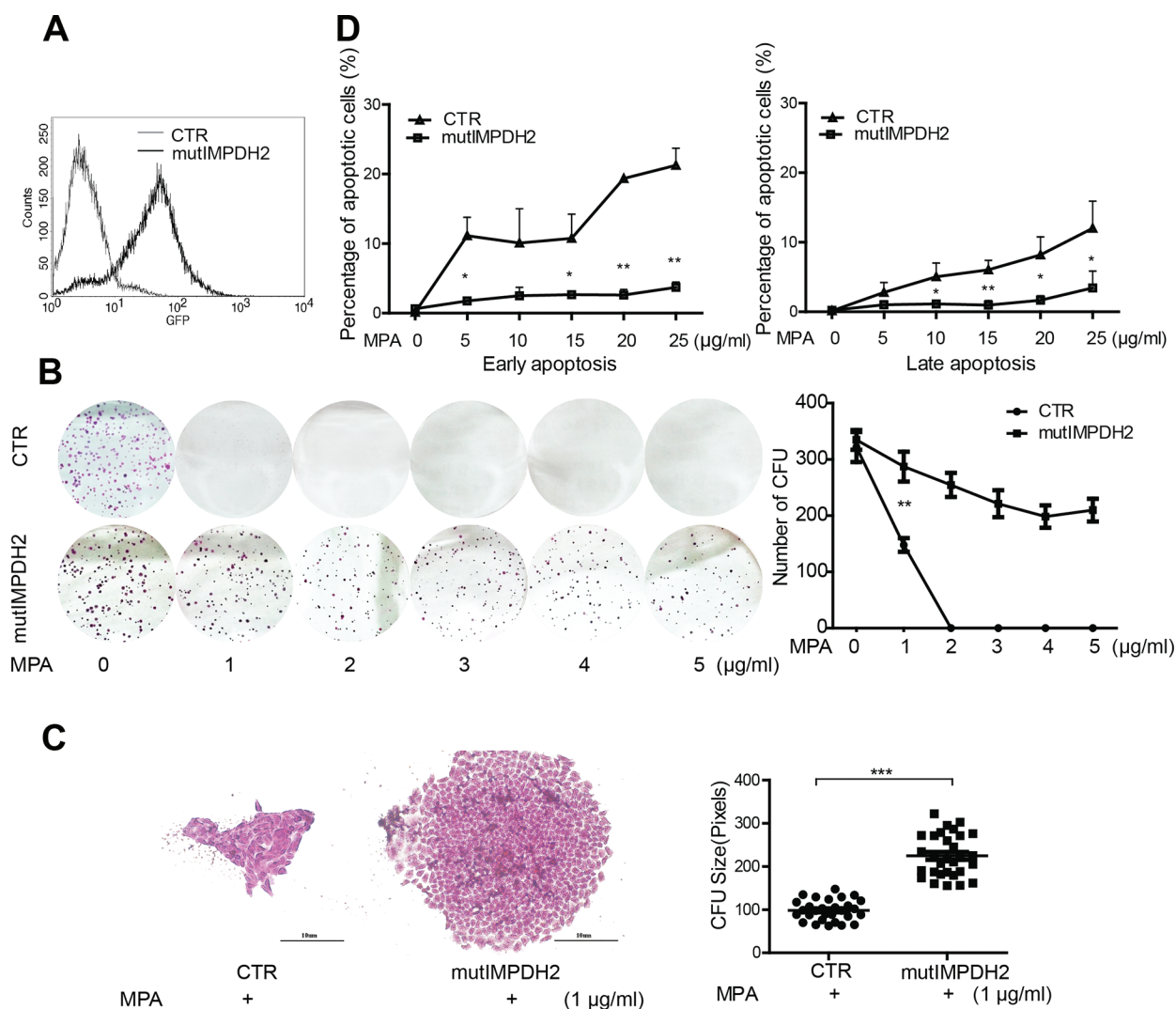
Figure 3. Force expression of a mutated IMPDH2, lacking the MPA-binding site, results in resistance to MPA. (A) An IMPDH2 variant having normal IMP hydrogenase activity but lacking the MPA-binding site was fused to a GFP reporter (mutIMPDH2) and expressed in HeLa cells by a lentiviral vector. FACS analysis showed robust GFP expression in the transduced HeLa cells, but not in mock-transduced cells. Transduced cells appear to be resistant to MPA both in (B) colony formation (mean ± SD, n = 6, **$P < 0.01$) and (C) cell proliferation assays (mean ± SEM, n = 30, ***$P < 0.001$). (D) MPA-mediated induction of early apoptotic cells, as well as late apoptotic cells, is reduced significantly in mutIMPDH2 HeLa cells (mean ± SD, n = 3. *$P < 0.05$; **$P < 0.01$).

delayed in the other mice (Figure 4B). Thus MPA counteracts growth of experimental tumors in this model.

Immunohistochemical staining of tumors harvested from these mice demonstrated significant downregulation ($P < 0.05$) of IMPDH2 at the protein level following treatment with MPA (Figure 4C). Concomitantly, MPA inhibited tumor cell proliferation, as shown by a significant reduction

($P < 0.05$) of proliferating cells assessed by the percentage of p-histone H3 positive cells (Figure 4D). Furthermore, MPA treatment provokes substantial apoptosis in the tumor cell compartment, as evidenced from the significant increase in the percentage of cleaved caspase-3-positive cells (Figure 4E). These results show that MPA counteracts tumor growth elicited by a fast-growing cancer cell *in vivo*.

Existence of Slow-Cycling Cancer Cells Compartment in Fast-Growing Tumors

Substantial evidence indicated that slow-cycling cancer cells can evade therapeutic agents and repropagate the tumor (18). To identify whether there are slow-cycling cancer cells in our experimental system, we established a lentiviral-based Tet-on label-retaining system that enables us to isolate slow-cycling
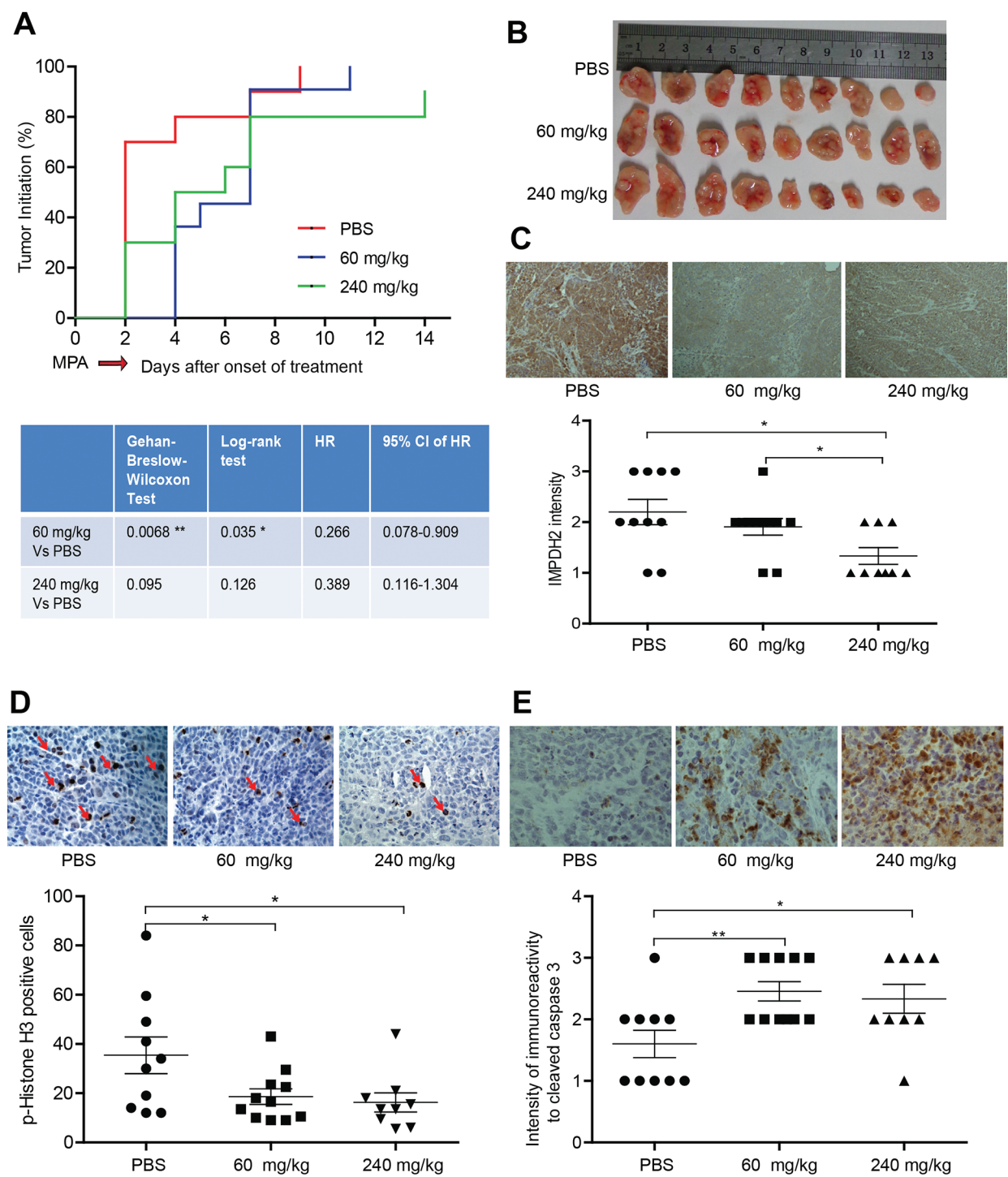
Figure 4. MPA delayed tumor initiation, inhibited cell proliferation and provoked tumor apoptosis in mice. (A) MPA treatment significantly delayed tumor initiation by HeLa cells in nude mice. (B) Following the experiment, animals were killed and tumors were harvested. The photograph illustrates the macroscopic appearance of the tumors in the respective groups. (C) Immunohistochemical staining of harvested tumor tissue sections revealed a significant downregulation of IMPDH2 protein levels following treatment with MPA. (D) Treatment of MPA significantly reduced the percentage of p-histone H3 positive (proliferating) cells in the tumors. (E) MPA treatment of HeLa-grafted nude mice significantly increased the numbers of anti-cleaved caspase-3 immunoreactive (apoptotic) cells (mean ± SEM, PBS, n = 10; 60 mg/kg, n = 11; 240 mg/kg, n = 9, *P < 0.05; **P < 0.01).
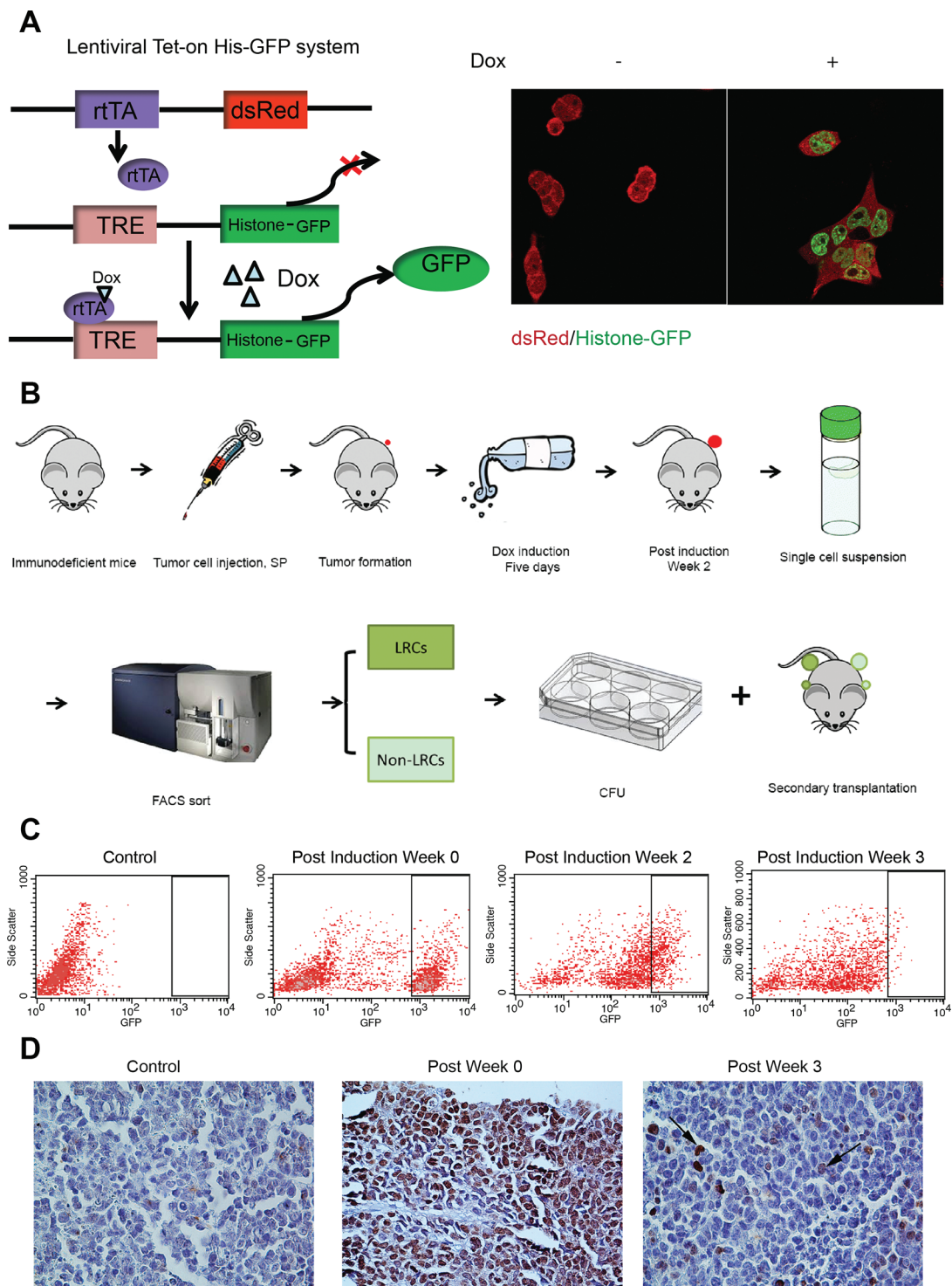
Figure 5. Identification of slow-cycling cancer cells using a lentiviral label-retaining system. (A) Illustration of principle; the lentiviral Tet-on histone-GFP strategy employed. Confocal imaging confirms the specific induction of nuclear histone-GFP expression in HeLa cells upon doxycycline treatment. (B) Schematic representation of the experimental approach to identify, isolate and characterize the slow-cycling cells, or termed as label-retaining cells (LRCs) *in vivo*. (C) FACS characterization of histone-GFP expression in transduced HeLa cells during 3 wks following release from doxycycline induction. (D) Immunohistochemical staining of harvested xenograft tumor tissues confirms the presence of nuclear anti-GFP immunoreactivity in these tissues.
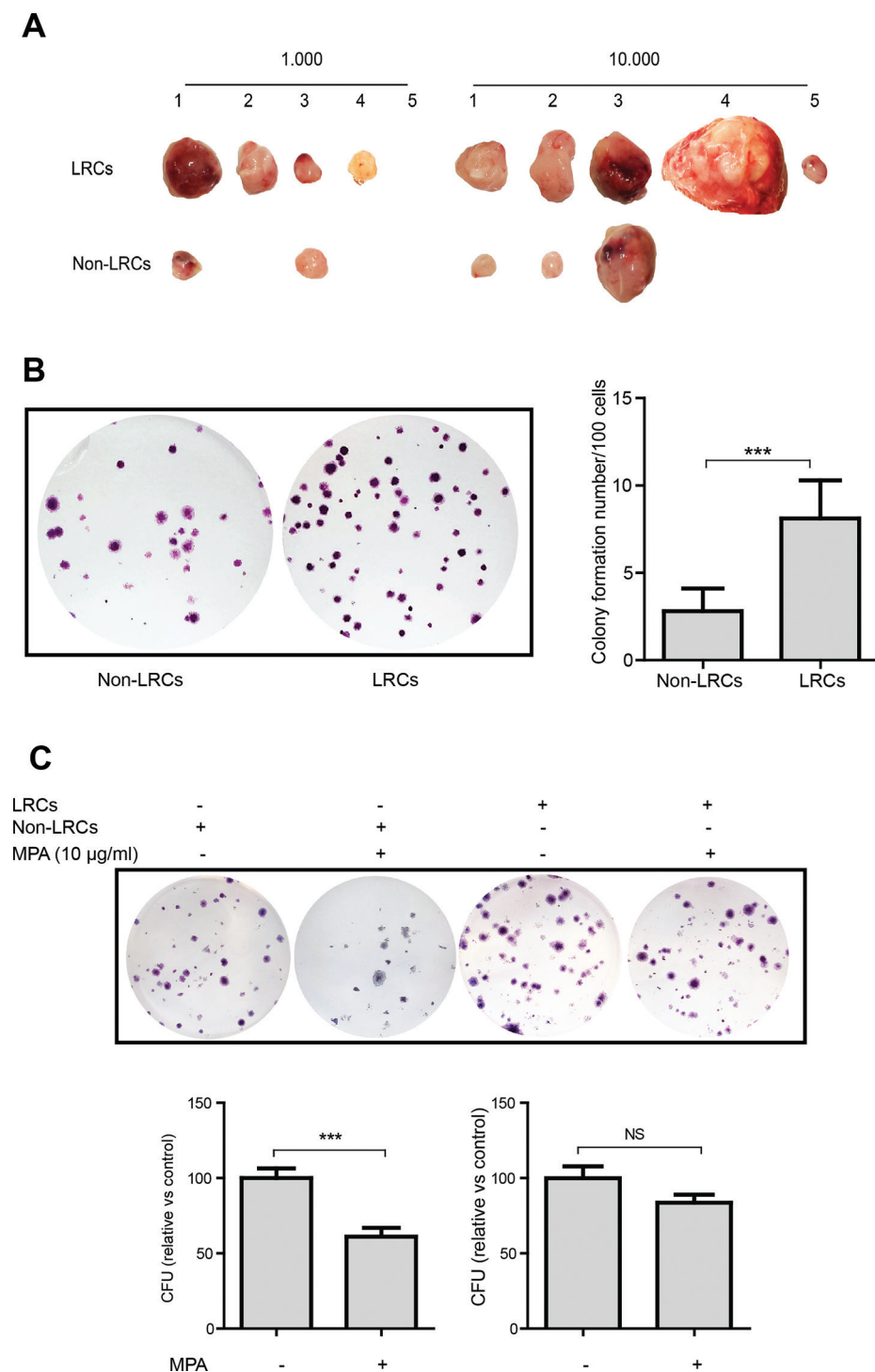
A

B

C

Figure 6. Grafted label-retaining cells are superior in tumor initiation and more resistant to MPA. (A) The macroscopic appearance of the tumors formed following secondary grafting of LRCs and non-LRCs, respectively. (B) Colony formation following grafting LRCs and non-LRCs harvested from xenograft tumor tissues (mean ± SEM, n = 19, ***P < 0.001). (C) Colony formation by LRCs and non-LRCs harvested from xenograft tumor tissues, when treated with MPA at a concentration of 10 μg/mL (mean ± SEM, n = 17, ***P < 0.001). NS, no signification.

cells for further functional characterization. To this end, cells were transduced with two vectors. One vector expresses a reverse Tet transactivator (rtTA), dsRed fluorescent protein and a neomycin-resistance cassette. The other vector expresses a histone-GFP fusion protein driven by a tetracycline response element (TRE) and puromycin-resistance gene (Supplementary Figure S1A). Stable cell lines can be established by cotransducing with these two vectors and the clones can be selected either via drug resistance or by cell sorting based on fluorescence. This constitutes a genotoxic free and cell proliferation-independent approach to identify slow-cycling cells. Upon induction by doxycycline, all the cells are labeled with GFP. After doxycycline withdrawal, dividing cells lose their GFP signal, whereas quiescent or slow-cycling cells retain their GFP expression, which thus serves as a label for LRCs (Figure 5A and Supplementary Figure S1).

HeLa cells engineered with histone-GFP[Tet-on] were subcutaneously engrafted in immunodeficient mice (Figure 5B). Once a small tumor was formed, histone-GFP expression was induced by doxycycline in the drinking water of the animal. Following doxy-cycline withdrawal, mice were killed at different time points. As shown by both FACS and immunohistochemical staining, a small population of LRCs was detected in tumors (Figures 5C,D). Thus we concluded that even fast-growing tumors harbor LRC compartment.

Slow-Cycling Cells Are Superior in Tumor Formation and Display More Resistance to MPA

To characterize LRCs functionally, LRCs and non-LRCs were isolated from HeLa cell-derived tumors using FACS sorter (Figure 5B and Supplementary Figure S3). Surprisingly, *ex vivo* CFU assay showed that LRCs were significantly more efficient in colony formation (non-LRCs: 2.8 ± 1.3 colonies/100 cells; LRCs: 8.1 ± 2.2, mean ± SEM, n = 19, P < 0.001) when compared with fast-cycling cells (Figure 6A). Consistently,

LRCs are more efficient in forming tumors, both with regard to size and number, in immunodeficient mice upon subcutaneous engraftment (Figure 6B).

Subsequently, we evaluated the relative sensitivity of LRCs and non-LRCs to MPA. Both populations were sorted and colony-forming potential was assessed in the presence or absence of MPA. Compared with the control groups, treatment with MPA (10 μg/mL) significantly inhibited the colony formation efficiency of non-LRCs but not of LRCs (where only minor effects were seen; Figure 6C). Thus, slow-cycling cancer cells when compared with fast-cycling cancer cells appear more resistant to MPA and may thus constitute the MPA-resilient reservoir in cancers.

DISCUSSION

IMPDH is a key enzyme in *de novo* guanine nucleotide biosynthesis and is thus a target for oncologic disease. MPA works as a potent IMPDH inhibitor that is used as an immunosuppressive drug (3). A phase I trial in patients with advanced multiple myeloma showed a positive correlation between clinical responses and depletion of the intracellular deoxyguanosine triphosphate levels by mycophenolate mofetil (MMF), the prodrug of MPA. MMF was administered up to a maximum dose of 5 g/day, which is two to three times higher than general use in organ transplantation patients, but was well tolerated in this study (19). In renal transplant patients, a tendency toward a lower risk of malignancy in MMF-treated patients versus non-MMF-treated has been reported in a large, prospectively conducted, observational cohort study (20). However, another clinical study in pancreatic cancer failed to show any beneficial effects (21). We found that only fast-cycling, but not slow-cycling, cancer cells are sensitive to the inhibitory effects of MPA. Thus, dissecting the heterogeneity of cancer may help to understand the distinct responsiveness to MPA treatment.

A unique aspect of this study is the use of a label-retaining technique that enables us to identify and isolate LRCs.

Classically, nucleotide analogs, such as 5-iodo-2′-deoxyuridine and bromodeoxyuridine, are used to identify LRCs. These agents can be used to identify LRCs, but the cells are not able to be isolated for functional study (22). Thus, fluorescent-coupled nucleotide analogs were developed for identification and isolation of LRCs. However, these agents are not competent for *in vivo* application (23). Although nucleotide analogs were also able to label cells *in vivo*, subsequent isolation of LRCs from the tissue is often a challenge that hampers further functional investigation (22). Another major drawback is that most of these labeling methodologies rely on cell division to label cells. Therefore, the real quiescent cells, in fact, cannot be labeled. Consequently, the introduction of modified nucleotides into cells profoundly alters the status of the cells (24). Integrating a lentiviral-based Tet-on cell-labeling system has circumstanced these limitations. Upon induction of the GFP fluorescent protein, all the cells can be labeled without genotoxic effect. It can be used for identification and isolation of slow-cycling cells both *in vitro* and *in vivo*. In this study, we used a histone-GFP fusion protein that localized in the cell nucleus with prolonged half-life (25). Thus, this technique bears broad implications for studying cell cycling. Indeed, we found the existence of a slow-cycling cancer cell compartment within the fast growing tumors formed by HeLa cells. These cells are superior in tumor initiation and more resistant to MPA. We speculate that the existence of slow-cycling cancer cells in different patient populations may affect the ultimate responsiveness of MMF/MPA treatment (19–21).

IMPDH2 is upregulated in proliferating cells (26), including in various types of cancer cells (27,28), and exhibits a five-fold higher sensitivity to MPA compared with IMPDH1. Mechanistically, the effect of MPA appears through inhibition of its canonical target, IMPDH2. Ectopic expression of a mutated *IMPDH2* (mut*IMPDH2*) largely nullifies the antiproliferative effects of MPA. Since IMPDH is the key

enzyme in the purine nucleotide synthesis pathway, we studied the effects of a modulating purine nucleotide pool on cell growth. Increasing the nucleotide concentration by supplementation of exogenous guanosine did not have a major effect on cell growth (Supplementary Figure S4). In addition, we found, surprisingly, that supplementation of exogenous guanosine counteracts the inhibitory effect of MPA only to a minor extent (Supplementary Figure S5). Although the antiproliferative effects of MPA are mainly dependent on targeting IMPDH2, depletion of nucleotides could only explain part of its mechanism of action.

Interestingly, a recent study has demonstrated a double functionality for IMPDH in Drosophila; in stress conditions, it can act as a transcription factor that inhibits cell proliferation (29). Thus, we speculate that IMPDH2 might be a ligand-regulated transcription factor and that MPA might act as a ligand. Indeed, IMPDH2 is located predominantly in cytoplasms in normal conditions of cultured HeLa cells, but efficiently translocated into the nucleus upon MPA treatment (Supplementary Figure S6A). Consistently, a mutated *IMPDH2* lacking the binding site of MPA was not able to translate into the nucleus, even with MPA treatment (Supplementary Figure S6B). These results appear to support the previous observation in Drosophila cells and our hypothesis. Furthermore, it is already known that MPA works as a ligand to activate the activity of peroxisome proliferator-activated receptors, such as PPARγ (30), a critical nuclear receptor on adipocyte differentiation. However, gene silencing of PPARα and PPARγ did not affect the sensitivity of HeLa cells to MPA treatment, excluding their potential involvement (Supplementary Figure S7). The scenario that MPA acts as a ligand for ligand-regulated transcription factors to regulate cancer cell growth is certainly interesting and therefore deserves further investigation.

In summary, this study demonstrated that through inhibiting IMPDH2, MPA was capable of constraining the growth

of fast-cycling cancer cells. Using a lentiviral Tet-on cell labeling technique, we identified slow-cycling cancer cells within the fast-growing tumors that are superior in tumor initiation, but more resistant to MPA. Thus, it is very necessary to develop regimens that can effective target slow-cycling cancer cells. Combining these regimens with agents targeting fast-cycling cancer cells, such as MPA, may be a viable option in cancer therapy.

CONCLUSION

Slow-cycling cancer cells within fast-growing tumors were identified. These cells, compared with fast-cycling cells, were superior in tumor initiation and resistant to IMPDH2 inhibition by MPA. Thus, simultaneous targeting of slow- and fast-cycling cells is necessary to eradicate cancer.

DISCLOSURE

The authors declare that they have no competing interests as defined by *Molecular Medicine*, or other interests that might be perceived to influence the results and discussion reported in this paper.

REFERENCES

1. Hanahan D, Weinberg RA. (2011) Hallmarks of cancer: the next generation. *Cell.* 144:646–74.
2. Natsumeda Y, *et al.* (1990) Two distinct cDNAs for human IMP dehydrogenase. *J. Biol. Chem.* 265:5292–5.
3. Carr SF, Papp E, Wu JC, Natsumeda Y. (1993) Characterization of human type I and type II IMP dehydrogenases. *J. Biol. Chem.* 268:27286–90.
4. Moosavi MA, Yazdanparast R, Sanati MH, Nejad AS. (2005) 3-Hydrogenkwadaphnin targets inosine 5′-monophosphate dehydrogenase and triggers post-G1 arrest apoptosis in human leukemia cell lines. *Int. J. Biochem. Cell. Biol.* 37:2366–79.
5. Guidicelli G, *et al.* (2009) The necrotic signal induced by mycophenolic acid overcomes apoptosis-resistance in tumor cells. *PLoS One.* 4:e5493.
6. Fellenberg J, Kunz P, Sahr H, Depeweg D. (2010) Overexpression of inosine 5′-monophosphate dehydrogenase type II mediates chemoresistance to human osteosarcoma cells. *PLoS One.* 5:e12179.
7. Fellenberg J, Bernd L, Delling G, Witte D, Zahlten-Hinguranage A. (2007) Prognostic significance of drug-regulated genes in high-grade osteosarcoma. *Mod. Pathol.* 20:1085–94.
8. Inai K, *et al.* (2000) Differentiation induction in non-lymphocytic leukemia cells upon treatment with mycophenolate mofetil. *Leuk. Res.* 24:761–8.
9. Takebe N, *et al.* (2006) IMP dehydrogenase inhibitor mycophenolate mofetil induces caspase-dependent apoptosis and cell cycle inhibition in multiple myeloma cells. *Mol. Cancer Ther.* 5:457–66.
10. Tressler RJ, Garvin LJ, Slate DL. (1994) Anti-tumor activity of mycophenolate mofetil against human and mouse tumors in vivo. *Int. J. Cancer* 57:568–73.
11. Govindasamy N, Murthy S, Ghanekar Y. (2014) Slow-cycling stem cells in hydra contribute to head regeneration. *Biol. Open.* 3:1236–44.
12. Schillert A, Trumpp A, Sprick MR. (2013) Label retaining cells in cancer—the dormant root of evil? *Cancer Lett.* 341:73–9.
13. Morris RJ, Potten CS. (1994) Slowly cycling (label-retaining) epidermal cells behave like clonogenic stem cells in vitro. *Cell Prolif.* 27:279–89.
14. Patel CG, Akhlaghi F. (2006) High-performance liquid chromatography method for the determination of mycophenolic acid and its acyl and phenol glucuronide metabolites in human plasma. *Ther. Drug Monit.* 28:116–22.
15. Chen K, *et al.* (2014) Rationale of personalized immunosuppressive medication for hepatocellular carcinoma patients after liver transplantation. *Liver Transpl.* 20:261–9.
16. Liang W, *et al.* (2012) Sirolimus-based immunosuppression in liver transplantation for hepatocellular carcinoma: a meta-analysis. *Liver Transpl.* 18:62–9.
17. Yam P, *et al.* (2006) Ex vivo selection and expansion of cells based on expression of a mutated inosine monophosphate dehydrogenase 2 after HIV vector transduction: effects on lymphocytes, monocytes, and CD34+ stem cells. *Mol. Ther.* 14:236–44.
18. Moore N, Houghton J, Lyle S. (2012) Slow-cycling therapy-resistant cancer cells. *Stem Cells Dev.* 21:1822–30.
19. Takebe N, *et al.* (2004) Phase I clinical trial of the inosine monophosphate dehydrogenase inhibitor mycophenolate mofetil (cellcept) in advanced multiple myeloma patients. *Clin. Cancer Res.* 10:8301–8.
20. Robson R, Cecka JM, Opelz G, Budde M, Sacks S. (2005) Prospective registry-based observational cohort study of the long-term risk of malignancies in renal transplant patients treated with mycophenolate mofetil. *Am. J. Transplant.* 5:2954–60.
21. Rodriguez-Pascual J, *et al.* (2013) A preclinical and clinical study of mycophenolate mofetil in pancreatic cancer. *Invest New Drugs.* 31:14–9.
22. Pan Q, *et al.* (2013) Identification of lineage-uncommitted, long-lived, label-retaining cells in healthy human esophagus and stomach, and in metaplastic esophagus. *Gastroenterology.* 144:761–70.
23. Xin HW, *et al.* (2013) Label-retaining liver cancer cells are relatively resistant to sorafenib. *Gut.* 62:1777–86.
24. Xin HW, *et al.* (2012) Tumor-initiating label-retaining cancer cells in human gastrointestinal cancers undergo asymmetric cell division. *Stem Cells.* 30:591–8.
25. Wang Y, *et al.* (2012) Identification of quiescent, stem-like cells in the distal female reproductive tract. *PLoS One.* 7:e40691.
26. Thomas EC, *et al.* (2012) Different characteristics and nucleotide binding properties of inosine monophosphate dehydrogenase (IMPDH) isoforms. *PLoS One.* 7:e51096.
27. Hager PW, Collart FR, Huberman E, Mitchell BS. (1995) Recombinant human inosine monophosphate dehydrogenase type I and type II proteins. Purification and characterization of inhibitor binding. *Biochem. Pharmacol.* 49:1323–9.
28. Zimmermann A, Gu JJ, Spychala J, Mitchell BS. (1996) Inosine monophosphate dehydrogenase expression: transcriptional regulation of the type I and type II genes. *Adv. Enzyme Regul.* 36:75–84.
29. Kozhevnikova EN, *et al.* (2012) Metabolic enzyme IMPDH is also a transcription factor regulated by cellular state. *Mol. Cell.* 47:133–9.
30. Makoto Ubukata, *et al.* (2007) Mycophenolic acid as a latent agonist of PPARr. *Bioorg. Med. Chem. Lett.* 17:4767–70.

Cite this article as: Chen K, *et al.* (2015) Differential sensitivities of fast- and slow-cycling cancer cells to inosine monophosphate dehydrogenase 2 inhibition by mycophenolic acid. *Mol. Med.* 21:792–802.